International Journal of Emerging Trend in Engineering and Basic Sciences (IJEEBS)
ISSN (Online) 2349-6967
Volume 2 , Issue 1(Jan-Feb 2015), PP244-250

Image Fusion using Wavelet Transform for Telemedicine

Patil Hanmant Venketrao[1], Dr. S. D. Shirbahadurkar [2]
[1](E&TC Department , NDMVP KBT COE,Nashik,India)
2(Principal, Dr DYP COE ,Ambi, Pune, India)

Abstract:- Image fusion means to integrate information from one image to another image. Medical images according to the nature of the images are divided into structural (such as CT and MRI) and functional (such as SPECT, PET). The purpose of MRI and PET images is adding structural information from MRI to functional information of PET images. The images decomposed with No subsampled Contour let Transform and then two images were fused with applying fusion rules. The coefficients of the low frequency band are combined by a maximal energy rule and coefficients of the high frequency bands are combined by a maximal variance rule. Finally, visual and quantitative criteria were used to evaluate the fusion result. In visual evaluation the opinion of two radiologists was used and in quantitative evaluation the proposed fusion method was compared with six existing methods and used criteria were entropy, mutual information, discrepancy and overall performance.
Keywords:- Image fusion, fusion rules, multiscale geometric analysis, nonsubsampled contourlet transform

I. INTRODUCTION

There are various types of medical images and each of them has specific application. Images such as MRI (Magnetic Resonance Imaging) and CT (Computed Tomography) provide anatomical information with high resolution, images such as PET (Positron Emission Tomography) and SPECT (Single Photon Emission Computed Tomography) provide functional information with low spatial resolution. Functional images don't have detailed anatomical information. To solve this problem, the physician can see two anatomical and functional images side-by-side. However, this is not a precise way, because the images have different resolutions, so researchers used image fusion in the medical field. Image fusion is the process of combining information from two or more images of a scene to construct an image that is more informative and is more suitable for visual perception.

Fig.1

Complex wavelet transforms (CWT)

The complex wavelet transform (CWT) is a complex-valued extension to the standard discrete wavelet transform (DWT). It is a two-dimensional wavelet transform which provides multiresolution, sparse representation, and useful characterization of the structure of an image. Further, it provides a high degree of shift-invariance in its magnitude. However, a drawback to this transform is that it is exhibits 2^d(where $d$is the dimension of the signal being transformed) redundancy compared to a separable (DWT).

The use of complex wavelets in image processing was originally set up in 1995 by J.M. Lina and L. Gagnon in the framework of the Daubechies orthogonal filters banks. It was then generalized in 1997 by Prof. Nick Kingsbury of Cambridge University.

Dual-tree complex wavelet transform (DTCWT)

The Dual-tree complex wavelet transform (DTCWT) calculates the complex transform of a signal using two separate DWT decompositions (tree a and tree b). If the filters used in one are specifically designed different from those in the other it is possible for one DWT to produce the real coefficients and the other the imaginary.

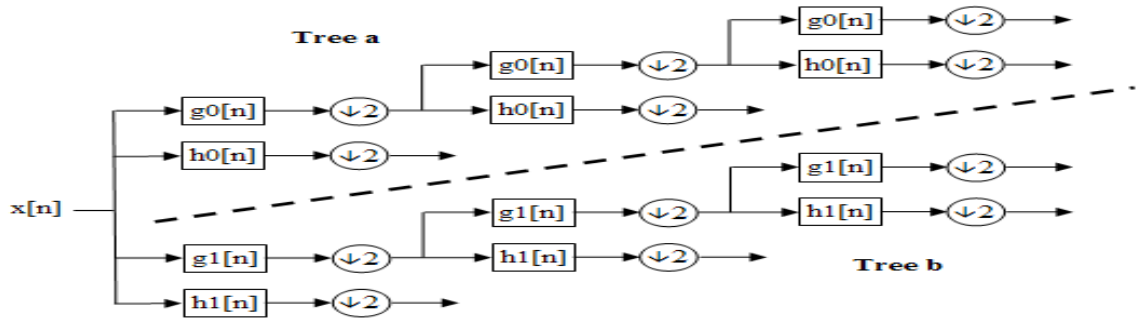

Fig. 2 : Block diagram for a 3-level DTCWT

This redundancy of two provides extra information for analysis but at the expense of extra computational power. It also provides approximate shift-invariance (unlike the DWT) yet still allows perfect reconstruction of the signal.

The design of the filters is particularly important for the transform to occur correctly and the necessary characteristics are:

- The low-pass filters in the two trees must differ by half a sample period
- Reconstruction filters are the reverse of analysis
- All filters from the same orthonormal set
- Tree a filters are the reverse of tree b filters
- Both trees have the same frequency response

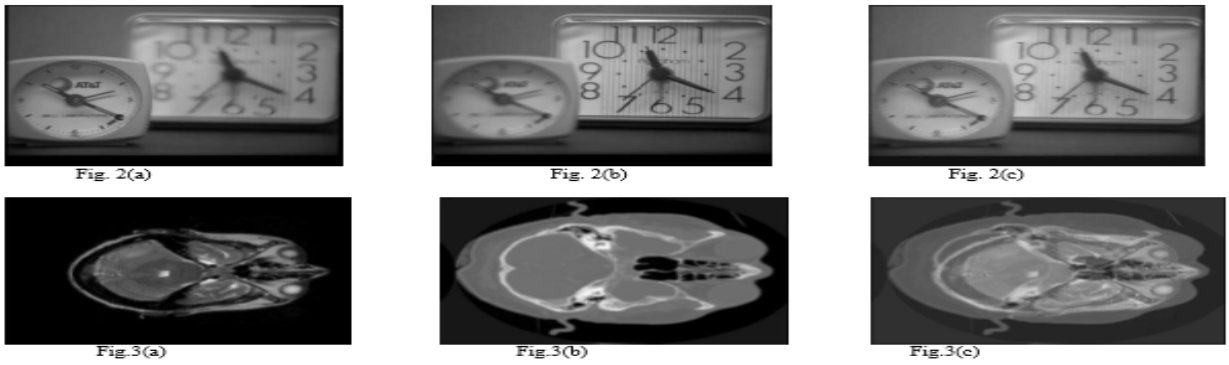

Fig. 3

Image Fusion Techniques and Quality Assessment Parameters for Clinical Diagnosis

A) Structural similarity index measure (SSIM)

The Structural similarity index measures follows that a measure of structural information change can provide a good approximation to perceived image distortion. The SSIM compares local patterns of pixel intensities that have been normalized such as luminance and contrast. It is an improved version of traditional

methods like PSNR and MSE. The SSIM index is a decimal value between 0 and 1. A value of 0 would mean zero correlation with the original image, and 1 means the exact same image
Symmetry: S(x, y) = S(y, x)
Boundedness: S(x, y) <= 1
Unique maximum: S(x, y) = 1 if and only if x = y (in discrete representations xi = yi, for all i = 1, 2,…….,N) SSIM can be calculated using SSIM

$$\text{Mean}\left(\frac{(2\mu_1\mu_2+C_1)(2\sigma_{12}+C_2)}{(\mu_1^2+\mu_2^2+C_1)(\sigma_1^2+\sigma_2^2+C_1)}\right) \quad \text{..... (2)}$$

Where $\sigma_1^2 = (A_{ij}^2.G) - \mu_1^2$

$\sigma_2^2 = (A_{ij}^2.G) - \mu_2^2$

$\sigma_{12}^2 = (A_{ij}\,B_{ij}\,G) - \mu_1.\mu_2$

$\mu_1 = A.G$ where G being Gaussian filter window i.e. ('gaussian', 11, 1.5)

$\mu_2 = B.G$

$C_1 = (K_1*L)^2$

$C_2 = (K_2*L)^2$ where L =255 and value of k varies from K = [0.01 0.03],

F.

B) Laplacian Mean Squared Error

B. Laplacian Mean Squared Error

Laplacian mean square error, error is calculated based on the laplacian value of the expected and obtained data is given by. LMSE is given by

$$\text{LMSE} = \frac{\sum_{i=1}^{m}\sum_{j=1}^{n}(\nabla^2 A-\nabla^2 B)^2}{\sum_{i=1}^{m}\sum_{j=1}^{n}(\nabla^2 A)^2} \quad \text{..... (3)}$$

G.

Laplacian operator is defined by the following expression.

$$\nabla^2 u = \left(\delta^2 u + \frac{\delta^2 u}{\delta^2 x\ \delta^2 y}\right)$$

Where u be defined as a function of (x, y).

Here each image pixel is subtracted from the average of the neighbouring pixels on the right, bottom, left and the top. This is considered the laplacian value of the particular pixel. The laplacian operator is denoted as,

$$\nabla^2 \mathbf{u} = \frac{(u_{i,j+1}+u_{i,j-1}+u_{i+1,j}+u_{i-1,j})-u\,ij}{4}$$

. For an ideal situation, the fused and perfect image being identical, the LMSE value is supposed to be 0. The error value which would exist otherwise would range from 0 to 1.

C) Mean Squared Error

Mean square error is a measure of image quality index. The large value of mean square means that image is a poor quality. Mean square error between the reference image and the fused image is

Where Ai, j and Bi, j are the image pixel value of reference image.

D) Peak signal to Noise Ratio

The ratio between maximum possible power of the signal to the power of the corrupting noise that creates distortion of image. The peak signal to noise ratio can be represented as

$$\text{PSNR (db)} = 20log\frac{255\sqrt{3mn}}{\sqrt{\sum_{i=1}^{m}\sum_{j=1}^{n}(A_{ij}-B_{ij})^2}}$$

Where A- fused image, B – perfect image, i – pixel pow index, j – pixel column index, M, N – Number of rows and columns respectively.

E) Entropy

Entropy is used to evaluate the information quantity contained in an image. The higher value of entropy implies that the fused image is better than the reference image. Entropy is defined as

$$E = -\sum_{i=0}^{L-1} pi\ log_2 p_i$$

Where L = total of grey labels, P = {p0, p1, ……..... pL-1} is the probability distribution of each labels

F) Structural Content

The structural content measure used to compare two images in a number of small image patches the images have in common. The patches to be compared are chosen using 2D continuous wavelet which acts as a low level corner detector. The large value of structural content SC means that image is poor quality

$$SC = \frac{\sum_{i=1}^{m}\sum_{j=1}^{n}(A_{ij})^2}{\sum_{i=1}^{m}\sum_{j=1}^{n}(B_{ij})^2}$$

G) Normalized Cross Correlation

Normalized cross correlation is a measure of similarity of two waveforms as a function of the time lag applied to one of them. The cross correlation is similar in nature to the convolution of two functions.

$$NCC = \sum_{i=1}^{m}\sum_{j=1}^{n}\frac{(A_{ij} * B_{ij})}{A_{ij}^2}$$

H) Maximum Difference

Difference between any two pixels such that the larger pixel appears after the smallest pixel. The large value of maximum difference means that image is poor in quality.

$$MD = \max[a_{ij} - a_{kl}] \quad i=1,2,\ldots,m \;\; j=1,2,\ldots,n$$

I) Normalized Absolute Error

The large value of normalized absolute error means that image is poor quality. NAE is defined as follows

$$NAE = \frac{\sum_{i=1}^{m}\sum_{j=1}^{n}(|A_{ij} - B_{ij}|)}{\sum_{i=1}^{m}\sum_{j=1}^{n}(A_{ij})}$$

J) Quality index (QI)

Quality Index of the reference image (R) and fused image (F) is given

$$QI = \frac{4\sigma_{ab}\,ab}{(a^2 + b^2)(\sigma_a^2 + \sigma_b^2)}$$

The maximum value Q=1 is achieved when two images are identical, where a & b are mean of images, s ab be covariance of R & F, σ_a^2 , σ_b^2 be the variance of image R,F

K) NWPM

The Normalized Weighted Performance Metric (NWPM) which is given

$$NWPM = \frac{\sum \forall_{i,j} Q_{ij}^{AF} W_{ij}^{A} + Q_{ij}^{BF} W_{ij}^{B}}{\sum \forall_{i,j} W_{ij}^{A} + W_{ij}^{B}}$$

TABLE 1 :Comparison between different Image Fusion methods

Parameter	Wavelet	DTCWT
PSNR	71.5754	75.4315
RMSE	112.2956	107.4193
QI	100	99.9998
NWPM	65.535	65.5349

Image fusion techniques can also be classified on the three main levels, including pixel level, feature level and decision level. Among the three fusion levels, pixel level fusion is the most encompassed and includes the majority of image fusion algorithms. Pixel-level algorithms work either in the spatial domain, such as averaging, PCA, Brovey and HSI, or in the transform domain, such as Multi-scale decomposition and Multi-geometric analysis. The spatial domain method usually leads to undesirable effects such as reduced contrast and spectral distortion. The advantage of the transform domain technique is that it can show salient features more clearly.

Multi-scale decomposition (MSD) methods don't have spatial domain problems such as spectral distortion and low contrast in the fusion result. Typical multi-scale decomposition includes the laplacian pyramid, 2-D wavelet transform. The laplacian pyramid has the distinguishing feature that each pyramid level generates only one bandpass image. Wavelet transform of images produces a non- redundant image representation and it can provide better spatial and spectral localization of image information as compared to other multi-resolution representations. However, 2-D wavelet transforms decompose images into only three directions (vertical, horizontal and diagonal), capturing only limited directional information. In order to overcome the limitations of the MSD methods, some novel multi-scale geometric analysis (MGA) tools have been introduced into image fusion that can capture 2-D geometrical structures in visual information much more effectively than MSD methods.

II. MULTI-SCALE GEOMETRIC ANALYSIS (MGA)

Typical multi-scale geometric analysis included the curvelet transform (CVT), contourlet transform (CT) and nonsubsampled contourlet transform (NSCT). Curvelet trans- form is effective in capturing curvilinear properties, like lines and edges. However, the curvelet transform in terms of computational is complex and time consuming. Contourlet transform can provide a multi-scale and direc- tional decomposition for images, which is more suitable for catching complex contours, edges and textures. Due to down- sampling and up-sampling, the contourlet transform is shift- variant. The nonsubsampled contourlet transform (NSCT) is a shift-invariant version of the contourlet transform. Shift-invariance is desirable in image analysis applications such as edge detection, contour characterization and image enhancement. Wang et al. used the NSCT transform for Multi-focus, CT-MRI and Visible-infrared images and also used the NMF algorithm for fusion rules in 2012. Wang et al. used the NSCT transform for Multi-focus, CT- SPECT and Visible-infrared images and they used three fusion rules.

Fig. 3. A 43-year-old man with unknown primary cancer origin. Axial slices by MR (a), PET (b), and a fused image (c) are shown. A swollen lymph node was observed in the left cervical region (not shown). Squamous cell carcinoma was identified by histopathological examination, but the primary tumor had not been detected. The location of the primary site was not confirmed by MR only, but left tonsillar cancer was suspected by fusion interpretation, because of its asymmetrical uptake (c: arrow), which was confirmed by surgery.

III. DISCUSSION

Normal structures in the head and neck area are basically symmetric, and abnormal structures including neoplasms are easily identified by a morphological modality only because of their asymmetry. Therefore, additional information by PET seemed unremarkable in many fresh cases. On the other hand, it is quite common for patients to have asymmetrical structures postoperatively. In addition, recurrent foci are often difficult to differentiate from postsurgery scar tissues, making it difficult in identifying recurrent tumors only by morphological modalities such as MR. For this reason, PET gave additional and helpful information in some suspected recurrent cases, in which MR interpretation did not yield accurate diagnoses.

Generally, there are two kinds of information obtained by FDG-PET, lesion characterization and navigation for detect- ing pathologic lesions by means of hypermetabolic state of glucose. In the head and neck area, FDG-avid lymph adenopathy develops by a nonspecific inflammatory process, and lymph adenopathy is sometimes difficult to differentiate from metastatic lymph node. Therefore, the role of lesion characterization by FDG-PET may be limited, and lymph nodes with FDG accumulation are not always metastatic. However, in this investigation, false-negative results for lymph node metastasis were problematic rather than false- positive findings, resulting in more underestimation of nodal involvement, as there were six under-staged cases and only one over-staged case by image fusion interpretation. This indicates that microscopic metastases cannot be diagnosed correctly both by PET and MRI, which is a usual limitation of diagnostic imaging. Among the under-staged cases by fusion interpretation, one case was accurately diagnosed by MR alone, because two metastatic lymph nodes were properly separated when interpreting T1-weighted images (N2b), but they were read as one positive node with focal intense uptake in interpreting T2-weighted and PET image fusion (N1).

In this analysis, MR and PET images were merged and registered manually on a workstation. The head and neck field is not likely to be influenced by respiratory motion if the patient's head is firmly fixed. Physiological uptake in the cerebellum or palatine tonsil can be used as landmark for image registration. There was no difficulty in making image fusion, and it took less than a few minutes to get fused images of appropriate quality for diagnosis, even using a manual procedure. Hardware-based fusion, like an inline PET/MR system, is not currently available, but the differ- ences between possible hardware-based fusion and our software-based approach might not be significant in the head and neck area for clinical application, although fused images can be even more easily obtained with more accurate registration.

It is known that the presence of synchronous cancer should be considered for patients with head and neck cancer. Nishiyama et al. reported that 11% of their head and neck cases had a simultaneous tumor, and five of six patients were diagnosed by FDG-PET. In our series, two patients had a past history of esophageal cancer; three patients had developed second oropharyngeal cancer during the follow-up period after treatment of initial head and neck cancer. In addition, lung cancer was newly diagnosed in one case.

IV. CONCLUSION

Image fusion from MR and PET may be useful in evaluating head and neck cancer. The additional value of image fusion may be minimal to fresh cases, but more equivocal lesions can be accurately diagnosed as positive in recurrent cases by interpreting fused images.

REFERENCES

1. F Maes, D Vandermeulen, P Suetens, Medical image registration using mutual information. Proceedings of the IEEE **91**(10), 1699–1721 (2003).
2. Y Wang, B Lohmann, Multisensor image fusion: concept, method and applications (Institute of Automatic Technology, University of Bremen, Bremen, Germany, 2000)
3. S Li, B Yang, Multifocus image fusion using region segmentation and spatial frequency. Image and Vision Computing **26**(7), 971–979 (2008).
4. H Li, BS Manjunath, SK Mitra, Multisensor image fusion using the wavelet transform. Graphical Models and Image Processing
5. K Amolins, Y Zhang, P Dare, Wavelet based image fusion techniques—an introduction, review and comparison. ISPRS Journal of Photogrammetry & Remote Sensing **62**(4), 249–263 (2007)
6. SL Cheng, JM He, ZW Lv, Medical image of PET/CT weighted fusion based on wavelet transform. Proceedings of the 2nd International Conference on Bioinformatics and Biomedical Engineering (iCBBE '08), 2008, 2523–2525
7. AS Lewis, G Knowles, Image compression using the 2-D wavelet transform. IEEE Transactions on Image Processing **1**(2), 244–250 (1992).
8. WZ Shi, CQ Zhu, Y Tian, J Nichol, Wavelet-based image fusion and quality assessment. International Journal of Applied Earth Observation and Geoinformation (2005).

I.